Phase separation and oxygen diffusion in electrochemically oxidized $La_2CuO_{4+\delta}$: A static magnetic susceptibility study

F. C. Chou
Center for Materials Science and Engineering, Massachusetts Institute of Technology, Cambridge, Massachusetts 02139

D. C. Johnston
Ames Laboratory and Department of Physics and Astronomy, Iowa State University, Ames, Iowa 50011

(Received 14 June 1995; revised manuscript received 5 February 1996)

The compound $La_2CuO_{4+\delta}$ is known to phase separate for $0.01 \lesssim \delta \lesssim 0.06$ below a temperature $T_{ps} \sim 300$ K into the nearly stoichiometric antiferromagnetic compound $La_2CuO_{4.01-4.02}$ with Néel temperature $T_N \sim 250$ K, and a metallic oxygen-rich phase $La_2CuO_{\approx 4.06}$ with superconducting transition temperature $T_c \approx 34$ K. We report studies of the superconducting and normal-state static magnetic susceptibility χ of $La_2CuO_{4+\delta}$ samples with $0 \lesssim \delta \lesssim 0.11$ prepared by electrochemical oxidation or reduction of conventionally synthesized ceramic $La_2CuO_{4+\delta}$. The upper limit to the miscibility gap at low T is found be $\delta \lesssim 0.065$, in agreement with the previous work. The interstitial oxygen diffusion during the phase-separation process was studied using thermal- and magnetic-field history-dependent $\chi(T,t)$ measurements versus temperature T and time t as a probe. Phase separation is found to be suppressed by quenching at $\gtrsim 100$ K/s and favored by slow cooling at ~ 0.5 K/min. A large thermal hysteresis of both the normal and superconducting state $\chi(T)$ was observed between data obtained after quenching to 5 K and then warming, and data obtained while or after slowly cooling from 300 K, for samples of $La_2CuO_{4+\delta}$ ($\delta \approx 0.030$, 0.044) within the miscibility gap. Quenching reduces T_c by ≈ 5 K relative to the value (34 K) obtained after slow cooling. A similar decrease is found for $La_2CuO_{4.065}$ which does not phase separate, indicating the importance of oxygen-ordering effects within this single phase. A model for the excess oxygen diffusion is presented, from which the data yield a nearly T-independent activation energy for excess oxygen diffusion of (0.24 ± 0.03) eV from 150 to 220 K apart from a possible anomaly near 210 K. [S0163-1829(96)04725-X]

I. INTRODUCTION

Phase separation has been found to occur in oxygen-doped $La_2CuO_{4+\delta}$,[1–3] as proved by Jorgensen *et al.* from a neutron-diffraction study of a polycrystalline sample of $La_2CuO_{4+\delta}$ ($\delta \sim 0.03$) synthesized under high oxygen pressure.[4] A reversible macroscopic phase separation was observed below a temperature $T_{ps} \approx 320$ K into two nearly identical orthorhombic phases with excess oxygen contents estimated[5] to be $\delta_1 \approx 0.01$ and $\delta_2 \approx 0.08$ at 200 K, respectively. The oxygen-rich metallic δ_2 phase becomes superconducting below $T_c \sim 34$–38 K,[4] whereas the oxygen-poor δ_1 phase exhibits long-range antiferromagnetic (AF) order below the Néel temperature $T_N \sim 250$ K.[3] Thermopower,[6–9] electrical resistivity,[6–10] magnetic susceptibility χ,[7,9,11] specific-heat,[9,11] and nuclear magnetic resonance/nuclear quadrupole resonance[12–15] (NMR/NQR) measurements have been found to show anomalies at T_{ps}. From neutron-diffraction measurements on a single crystal with $\delta \approx 0.03$, the excess oxygen was found to be located in interstitial sites between adjacent LaO layers, tetrahedrally coordinated by four La atoms.[16,17] In Ref. 17, the authors concluded that the miscibility gap boundaries at 15 K were $\delta_1 \approx 0$ and $\delta_2 \sim 0.048$. NMR/NQR studies of single crystals produced under high oxygen pressure indicate that the miscibility gap boundaries below ~ 200 K are $\delta_1 \approx 0.01$ and $\delta_2 \approx 0.06$.[13,15,18] Ryder *et al.* have presented dark-field transmission-electron microscope images which revealed an anisotropic herringbone-type domain structure of the oxygen-rich and -poor phases of characteristic minimum dimension 300–1500 Å.[9]

It has recently become possible to synthesize homogeneous polycrystalline[19–28] and single crystal[26,27,29] $La_2CuO_{4+\delta}$ samples with controlled variable composition $\delta \lesssim 0.12$ by electrochemically oxidizing La_2CuO_4 in aqueous base at ambient temperature. This synthesis technique has allowed a detailed study of the phase diagram in the (T-δ) plane. Neutron-diffraction measurements of the miscibility gap limits using such samples[30] were in agreement with the above values found from NQR/NMR and the maximum T_{ps} was found to be about 415 K for $\delta \approx 0.03$, as shown in the phase diagram for $\delta < 0.07$ in Fig. 1.[6,30–34] Samples with $\delta = 0.08$ to 0.12 showed no phase separation down to 10–16 K demonstrating that these compositions are beyond the upper miscibility gap limit $\delta \approx 0.06$.[35]

In order for macroscopic phase separation to occur below T_{ps} in the $La_2CuO_{4+\delta}$ system for compositions δ within the miscibility gap, the excess oxygen ions (and their doped holes) must obviously diffuse distances large compared to the unit cell dimensions. On the other hand, the excess oxygen ions should also become frozen in place at sufficiently low temperatures. On the basis of ^{139}La spin-lattice relaxation rate data, Hammel *et al.* concluded that the mobility of the excess oxygen becomes insufficient below ~ 190–200 K to allow macroscopic phase separation to proceed.[15,18] In contrast, Ryder *et al.*[9] have also explained their observed hysteresis in the resistivity between 150 and 280 K, obtained on slowly cooling and warming (0.2 K/min), as due to phase separation, and they concluded that diffusion of the excess

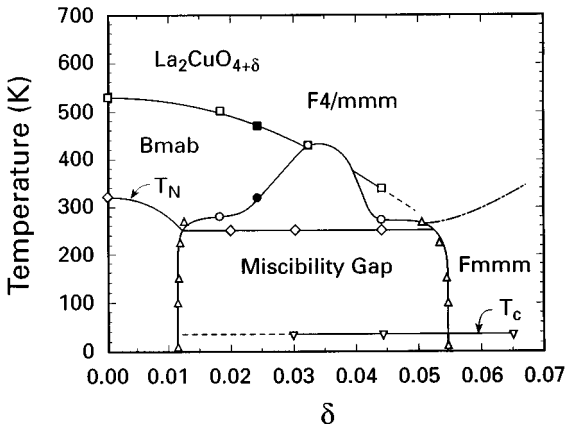

FIG. 1. Structural, magnetic, and superconducting phase diagram of $La_2CuO_{4+\delta}$. The structural phase diagram is from Ref. 30. The Néel temperature T_N=325–328 K for La_2CuO_4 (δ=0) is from Refs. 6, 31, and 32, and the parabolic dependence of T_N on doping level for δ<0.012 is from Refs. 33 and 34.

oxygen is significant down to ≈150 K.

The superconducting and normal-state properties below T_{ps} of phase-separated compositions of $La_2CuO_{4+\delta}$ are expected, and found,[3,6,7,9,13,15,18,23,28,30,36–46] to depend on the thermal history of the samples. Many workers[3,9,13,15,18,28,30,37,38,40–43] have found that the superconducting T_c of samples quenched to ~4 from 300 K is depressed by ~5 K compared with that (~32–34 K onset) for slowly cooled samples. For example, after quenching to ~4 K subsequent annealing at a temperature T_{ann} followed by quenching to 4 K results in a maximum T_c onset of ≈32 K for T_{ann}≈200 K, where the diamagnetic shielding susceptibility at 5 K was found to be independent of T_{ann}; higher or lower T_{ann} values resulted in a reduced T_c.[13,18] In a related experiment, samples were first cooled to ~4 K, heated to T_{ann}, then slowly cooled in H≈100 Oe to low T; in this case, the Meissner fraction showed a large increase for T_{ann} in the range 200–220 K and saturated above 220 K, with a concommitant increase in T_c onset from 34 to 40 K for T_{ann} increasing from 160 to 220 K.[36] By comparing ac susceptibility and (dc) Meissner effect data, Sulpice *et al.*[37] concluded that the enhanced Meissner effect at 4 K in H=10 Oe, which they found upon increasing T_{ann} from 220 to 270 K, resulted from flux-pinning effects and not from an increase in the superconducting volume. In contrast, it was inferred from low-field microwave absorption measurements at 10 K following a quench to 10 K and annealing at T_{ann} for 10 min followed by slow cooling that the superconducting volume was enhanced for T_{ann}≳170 K.[45] The intensity of a Cu^{+2} electron-spin-resonance signal observed for quenched samples at 4.2 K decreased markedly for 180 K≤T_{ann}≤220 K.[46] Kremer and co-workers[39–41] found that samples quenched to 5 from 300 K exhibit only a small superconducting diamagnetism, and that subsequent annealing at T_{ann}=150–300 K caused the apparent superconducting volume to increase in two steps with increasing T_{ann}. A small maximum in the apparent superconducting volume was found when T_{ann}≈180 K; a further and much larger maximum was observed for T_{ann}≈220 K. These authors believe that the excess oxygen does not diffuse below ~200 K, and therefore interpreted the first step as arising from coalescence into percolating superconducting clusters of ferromagnetic polarons (ferrons) associated with the doped holes in the CuO_2 planes, not accompanied by motion of the excess oxygen, and the second step as arising from macroscopic phase separation involving the excess oxygen. Because the first step was assumed not to involve oxygen diffusion, Kremer *et al.* concluded that the phase-separation transition is electronically driven. Perhaps surprisingly, several studies have also suggested a magnetic-field history dependence to the superconducting properties for δ≲0.02,[36,39] again consistent with an electronic mechanism for phase separation; these results have not been confirmed.[37]

Further investigation of the excess oxygen diffusion process is desirable in order to better understand how to interpret the reported thermal and magnetic-field history-dependent physical properties of the $La_2CuO_{4+\delta}$ system. In this paper, we report detailed measurements of the dependences of the superconducting and normal-state dc magnetization M and magnetic susceptibility χ on cooling rate, annealing temperature after quench to 5 K, magnetic field H and time t for $La_2CuO_{4+\delta}$ samples with δ≈0.02, 0.030, and 0.044, which lie within the miscibility gap region, and δ≈0.00, 0.065, and 0.110 which are outside the miscibility gap region. The results of these experiments are interpreted in terms of a model for the excess oxygen diffusion, driven by the mechanism of phase separation.

II. EXPERIMENTAL DETAILS

A. Sample preparation and characterization

Polycrystalline $La_2CuO_{4+\delta}$ samples with δ≈0.030(10), 0.044(10), 0.065(10), and 0.110(10) were prepared by electrochemically oxidizing conventionally prepared ceramic La_2CuO_4 as described previously.[22,35] Additionally, a sample with minimum excess oxygen content was prepared by electrochemically *reducing* ceramic La_2CuO_4 with a current of 100 μA for one week. From $\chi(T)$ measurements, this electrochemically reduced sample showed a Néel temperature T_N≈315 K, which corresponds to δ<0.005 according to Refs. 33 and 47, and no trace of superconductivity from low-field (10–50 Oe) dc magnetization measurements. A ceramic sample of $La_2CuO_{4+\delta}$ conventionally prepared in oxygen was also studied. This sample showed a trace of superconductivity below 26 K upon field cooling in an applied magnetic field H=50 Oe, and has an excess oxygen content estimated from Fig. 1 to be δ≈0.02.

The oxygen contents of the electrochemically treated samples were calculated from the weight loss of $La_2CuO_{4+\delta}$ powder under He atmosphere in a Perkin Elmer Series 7 thermogravimetric analyzer between 180 and 380 °C.[22,35] The samples with δ≈0.044 and 0.065 are from the same batches that were examined by neutron-diffraction structural analysis.[30,35] The sample with δ≈0.044 shows a tetragonal-to-orthorhombic ($F4/mmm$ to $Fmmm$) structural transition at about 340 K and then a phase-separation transition below T_{ps}≈270 K into two orthorhombic phases described by space groups $Fmmm$ (75%) and $Bmab$ (25%).[30] The sample with δ≈0.065 shows a single $Fmmm$ structure with no phase separation down to 10 K (see Fig. 1).[35]

B. Magnetic susceptibility measurements and quenching procedures

Temperature- (T) dependent dc magnetic susceptibilities $\chi(T)$ and superconducting transition temperatures T_c were measured using a Quantum Design superconducting quantum interference device (SQUID) magnetometer. The scan length was 4 cm for all measurements. Samples of $La_2CuO_{4+\delta}$ were quenched from $\approx$300 K directly into liquid nitrogen at 77 K and quickly transferred to the precooled SQUID magnetometer at 5 K in zero applied magnetic field H. Alternatively, samples were inserted directly into the precooled magnetometer at 5 K from ambient temperature. The average quenching rate is estimated to be $\gtrsim$100 K/min. No significant differences were found for either the superconducting or normal-state magnetic properties between these two quenching procedures. The susceptibilities after quenching, $\chi^Q(T)$, were measured upon warming. The susceptibility data measured while slowly cooling, $\chi^{SLC}(T)$, were obtained upon cooling from $\approx$300 K in temperature steps of 5 or 10 K. There was a momentary undercool of about 5 to 15 K below the set temperature for data taken on cooling. The average cooling rate for the discrete slow cooling process was 0.4–0.7 K/min. The time for the sample chamber temperature to stabilize at a new temperature for warming and cooling experiments is estimated to be about 4 and 10 min, respectively. The measuring time to obtain each M value was $<$30 sec. Ferromagnetic impurity contributions of $\sim$(8.4 to 10.8)$\times10^{-5}$ G cm^3/g, equivalent to the magnetization of $\sim$3 at. ppm of Fe metal impurities with respect to Cu, were determined by extrapolating linear fits to the $M(H)$ isotherm data to $H=0$ from $H>1.5$ T at 300 K; these contributions were corrected for in the $\chi(T)$ data presented below. Superconducting properties were measured at low field ($H=10$ Oe) on warming, either after quenching or slow cooling; to minimize the remanant field of the magnet, the magnet was quenched before each such measurement.

To measure the t dependence of χ at a fixed T, a sample was first quenched to 5 K in zero applied field as described above. The T was then quickly raised to the minimum measurement T and $\chi(t)$ measured for about 1 h. After measurements at the initial minimum T, subsequent measurements at higher T in increments of 5 or 10 K were made after heating from the last measurement T.

III. EXPERIMENTAL RESULTS

A. Miscibility gap

According to proposed T-δ phase diagrams for $La_2CuO_{4+\delta}$,[13,15,18,23,28,30] our samples with $\delta\approx0.030$ and 0.044 are expected to be separated below T_{ps} into two phases with compositions at the miscibility gap boundaries $\delta_1\approx0.01$ and $\delta_2\approx0.06$, respectively. On the basis of previous work cited above, the δ_1 phase is antiferromagnetic with $T_N\sim250$ K, whereas the δ_2 phase is superconducting with $T_c=32$–34 K. Our samples with $\delta\approx0.065$ and 0.110 do not phase separate according to the previous neutron-diffraction results on these samples,[35] whereas $T_{ps}\approx270$ K for the $\delta\approx0.044$ sample.[30]

Figure 2 shows $\chi(T)$ data for four samples of $La_2CuO_{4+\delta}$ with $\delta\approx0.02$, 0.030, 0.044, and 0.065. The data for $\delta\approx0.030$ and 0.044 were obtained upon warming, after slowly cooling in order to maximize phase separation, whereas the data for the other two samples were measured upon warming after quenching to 5 K.

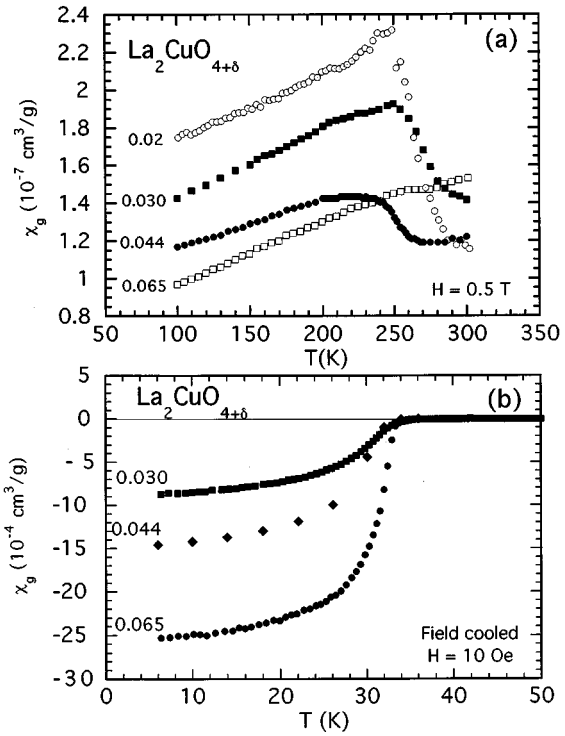

FIG. 2. (a) Normal-state magnetic susceptibilities χ_g versus temperature T for $La_2CuO_{4+\delta}$ samples with $\delta\approx0.02$, 0.030, 0.044, and 0.065, measured in an applied magnetic field $H=0.5$ T. (b) Magnetic susceptibility χ_g versus temperature T for the $La_2CuO_{4+\delta}$ samples with $\delta\approx0.030$, 0.044, and 0.065. The data were measured at $H=10$ Oe upon warming after field cooling.

The normal-state $\chi(T)$ data are shown in Fig. 2(a). The pronounced peaks in $\chi(T)$ at $T_N\approx250$ K, associated with AF ordering of the δ_1 phase and plotted in Fig. 1, are seen to decrease in magnitude with increasing δ and to essentially disappear by $\delta\approx0.065$. This indicates that the upper miscibility gap composition at $T\sim250$ K is $\delta_2\leqslant0.065$, consistent with the structural data in Fig. 1. From Fig. 2(a), the peak in $\chi(T)$ due to the AF δ_1 phase becomes rounded with increasing δ, particularly for the $\delta=0.044$ sample; a very similar $\chi(T)$ behavior was observed[11] for a single crystal with[48] $T_{ps}=(260\pm5)$ K and $T_N=(245\pm3)$ K. This evolution makes it difficult to separate the effects on $\chi(T)$ due to phase separation and AF ordering of the δ_1 phase for the more heavily doped samples. The evolution in the shape of the anomaly with increasing δ suggests a reduction in the domain size of the δ_1 phase with increasing δ within the miscibility gap region.

According to Fig. 1, the minimum T_N observed for the $La_2CuO_{4+\delta}$ system should be $\approx$250 K. However, from magnetization ($T_N=0$–300 K),[33] ($T_N=130$ K),[49] ($T_N=135$–305 K),[50] ($T_N=32$–310 K),[51] muon spin rotation ($T_N=10$–300 K),[52] and neutron diffraction ($T_N=45$–295 K) (Ref. 53) measurements, T_N values less than 50 K have been observed.[54] These low values are presumably associated with the presence of cation vacancies, impurities and/or nonequilibrium excess oxygen contents or distributions in particular samples.

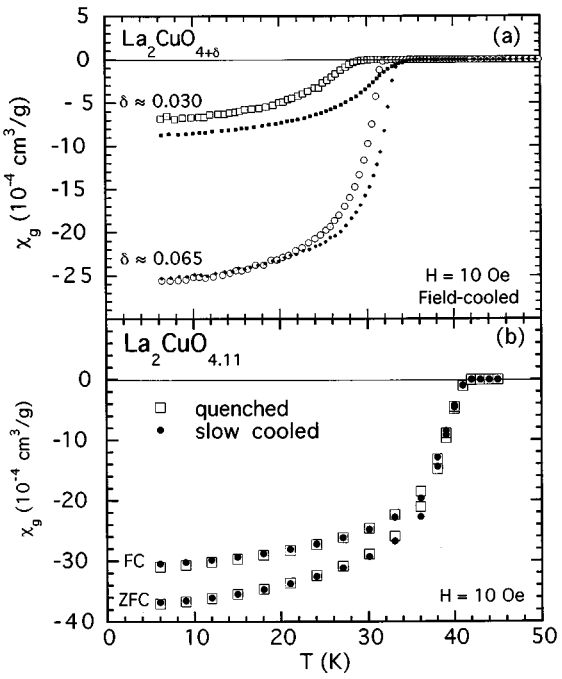

FIG. 3. Magnetic susceptibility χ_g of $La_2CuO_{4+\delta}$ samples in an applied field $H=10$ Oe versus temperature T, for (a) $\delta\approx0.030$ and 0.065 and (b) 0.11. The samples were either quenched (open symbols) or slowly cooled (filled symbols) from 295 to 5 K in $H=10$ Oe prior to measurement on warming.

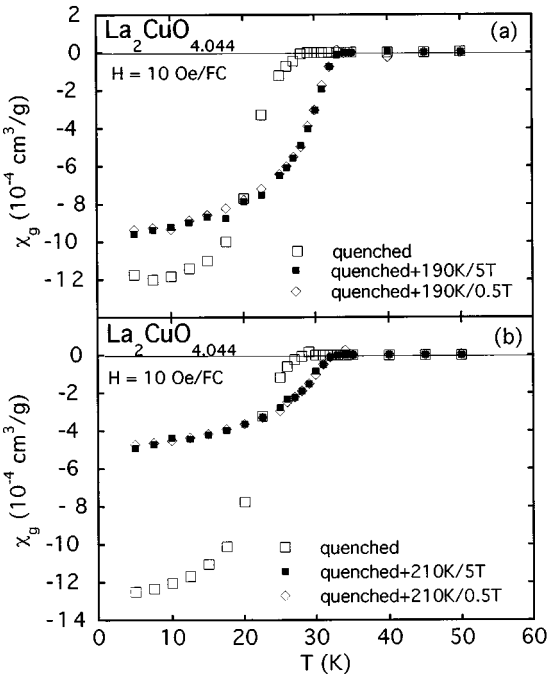

FIG. 4. Magnetic susceptibility χ_g of $La_2CuO_{4.044}$ in an applied field $H=10$ Oe versus temperature T. The samples was first quenched from 300 to 5 K in $H=10$ Oe and $\chi(T)$ measured on warming (open squares). Then the sample was annealed for 1 h in $H=0.5$ T (diamonds) or 5 T (filled squares) at a temperature T_{ann} of 190 K (a) or 210 K (b), quenched again to 5 K in $H=10$ Oe, and $\chi(T)$ remeasured on warming.

Information about the miscibility gap was also obtained from superconducting state $\chi(T)$ data. Shown in Fig. 2(b) are $\chi_g(T)$ data for the $La_2CuO_{4+\delta}$ samples with $\delta\approx0.030$, 0.044, and 0.065. These data were obtained on warming after slowly field cooling the samples in $H=10$ Oe from ≈295 K. The measured field-cooled χ values are good indicators of change of the superconducting volume fraction, when demagnetization factor, density of pinning center, and penetration depth are assumed to be the same in these samples. The measured χ(5 K) values of the superconducting δ_2 phase increase monotonically with increasing δ, whereas the T_c of this phase, plotted in Fig. 1, is nearly constant at 32–34 K. These data are consistent with the miscibility gap boundaries $\delta_1\approx0.01$–0.02 and $\delta_2\approx0.06$ in Fig. 1.

B. Thermal and magnetic-field history dependence of T_c and of the superconducting fraction

The superconducting state magnetic susceptibilities $\chi_g(T)$ measured with $H=10$ Oe for $La_2CuO_{4+\delta}$ samples with $\delta\approx0.030$, 0.065, and 0.11 are shown in Fig. 3. For each sample, data are presented both after quenching and slow cooling from 295 K. For $\delta\approx0.030$, which is within the miscibility gap, the field-cooled data in Fig. 3(a) show that the slowly cooled sample has both a larger T_c (by ≈5 K) and diamagnetic susceptibilities than the quenched sample. On the other hand, for $\delta\approx0.065$, which shows no phase separation according to neutron-diffraction analysis,[35] the sample obtained after slowly cooling has a higher T_c (by ≈2 K) but almost no superconducting fraction change, compared with the quenched sample. The data in Fig. 3(b) for $\delta\approx0.110$, which also does not exhibit phase separation,[35] show no difference in the superconducting properties between quenching and slow cooling. Similar thermal history dependences of T_c have been observed previously for samples of $La_2CuO_{4+\delta}$ with δ within the miscibility gap.[3,9,13,15,18,28,30,37,38,40–43] We conclude that this thermal hysteresis effect on T_c observed in phase-separated samples arises at least in part from the hysteretic effect in the pure $La_2CuO_{4.065}$ phase in those samples. The latter behavior may in turn reflect thermal history-dependent oxygen ordering effects, consistent with the neutron-diffraction data for the $La_2CuO_{4.065}$ sample which showed superlattice reflections presumably associated with spatial ordering of the excess oxygen atoms.[35]

We have carried out several experiments on $La_2CuO_{4.044}$ to study whether the superconducting properties depend on the magnetic-field history.[36,39] The superconducting state $\chi_g(T)$ data in Fig. 4 were obtained after quenching to 5 K in a 10 Oe field and also after annealing at 190 K [Fig. 4(a)] or 210 K [Fig. 4(b)] for 1 h in fields of 0.5 or 5 T, and then field cooling to 5 K in a field of 10 Oe. The superconducting state data in Fig. 4 show no observable dependence on the field at which the annealing at 190 or 210 K was carried out. Thus, these measurements do not confirm the field dependences of the superconducting properties reported for $\delta\lesssim0.02$ in Refs. 36 and 39.

C. Time dependence of the normal-state magnetic susceptibility at fixed temperature

The time t evolution at fixed temperature T of the magnetic susceptibility χ for $La_2CuO_{4.044}$ was measured after ini-

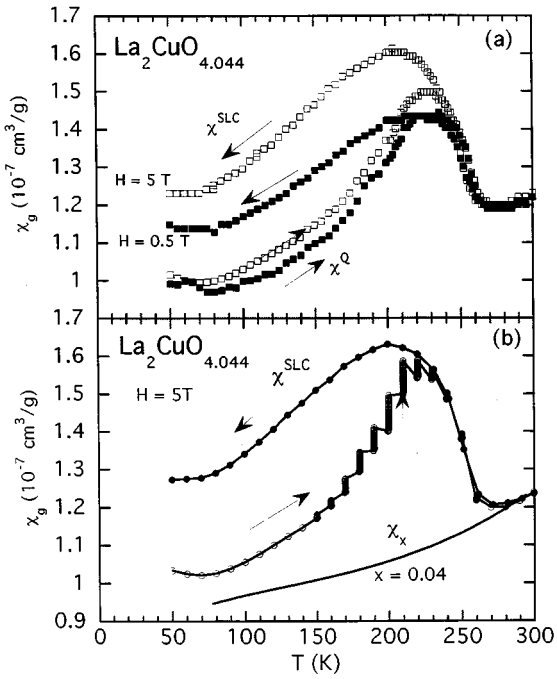

FIG. 5. (a) Normal-state magnetic susceptibility χ_g vs temperature T for $La_2CuO_{4.044}$. The sample was zero-field quenched from ≈295 to 5 K first and then measured at $H=0.5$ or 5 T upon warming, yielding $\chi^Q(T)$ data. After the $\chi^Q(T)$ data were obtained at a given field up to 300 K, data were obtained upon slowly cooling in T increments of 5 K, as indicated, denoted by $\chi^{SLC}(T)$. (b) Magnetic susceptibility χ_g of $La_2CuO_{4.044}$ versus temperature T, at an applied field $H=5$ T measured upon warming after quenching to 5 K (open circles), or while slowly cooling from 295 K (filled circles). The multiple data points for constant $T\geqslant 150$ K reflect the time dependence of χ_g measured over a period of about 11 h. Data for $La_{1.96}Sr_{0.04}CuO_4$ from Ref. 57 (lowest solid curve), $\chi x(T)$ in Eqs. (11)–(13), represent the behavior expected for $La_2CuO_{4.044}$ in the absence of phase separation.

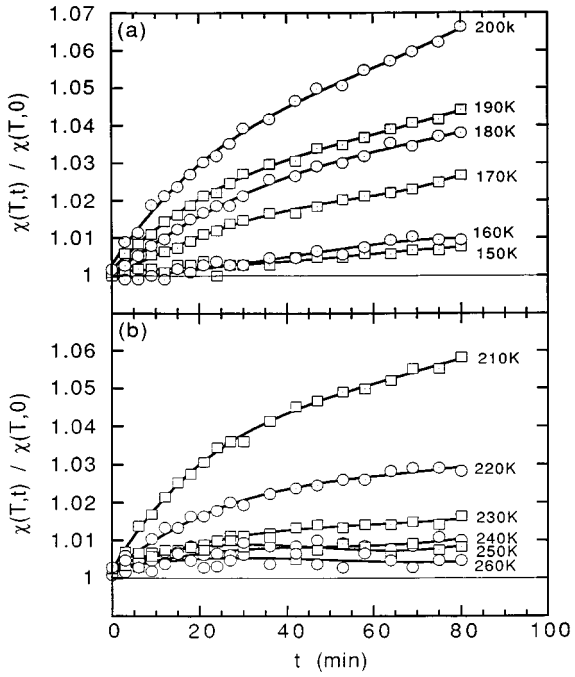

FIG. 6. The time t evolution of the magnetic susceptibility $\chi(t)/\chi(0)$ of $La_2CuO_{4.044}$ after quenching from ~300 to 5 K and heating to successive constant temperatures (a) $T=150$–200 K, (b) $T=210$–260 K. For clarity, only a representative fraction of the data is shown.

tially quenching the sample to 5 K and then rapidly heating the sample to the first (lowest) measurement T. $\chi(T,t)$ data were measured at this T for about 1 h. The sample was then repeatedly heated to the next higher measurement T, which was either 5 or 10 K above the previous one, and the measurement repeated. A typical complete measuring cycle for $H=5$ T is shown in Fig. 5(b). Note that at a given measurement T, this sequence preserves the previous time evolutions in the sample at lower measurement temperatures.

For an ideal quench, one would expect $\chi^Q(T)$ in Fig. 5(a) to be due to the supersaturated system containing a homogeneous distribution of excess oxygen. However, the anomalies between 150 and 260 K observed in the $\chi^Q(T)$ data in Fig. 5(a), reflecting long-range AF order, indicate that phase separation has occurred in the quenched sample. The most probable explanation is that our quenching rate is not fast enough to completely prevent phase separation; evidence for this is the slight positive curvature in $M(H)$ for $H>0.3$ T for the quenched sample of $La_2CuO_{4.044}$ (not shown). The distinct positive curvature in $M(H)$ for $H\gtrsim 3$ T for the slowly cooled sample signals the transition into the weak ferromagnetic (WFM) state with increasing H, consistent with the occurrence of phase separation in this sample. On the other hand, the quenched sample shows a more nearly linear $M(H)$ behavior, suggesting that the phase-separation transition is suppressed in this sample. A second major contributing factor is that even if the quench to 5 K is ideal, phase separation occurs during the $\chi^Q(T)$ measurement upon heating due to unfreezing of the excess oxygen above ~150 K (see below), resulting in the formation of an AF phase which then shows a $\chi(T)$ anomaly at T_N ~250 K.

The measured t dependences of χ at $H=5$ T for $La_2CuO_{4.044}$ at each fixed T from 150 to 290 K are shown in Fig. 6. For 150 K$\leqslant T\leqslant$260 K, $\chi(T,t)$ increases with t, but the 1 h measurement time at each T is not long enough for χ to grow to the equilibrium $\chi^{SLC}(T)$ values (see Fig. 5). The slight decrease in $\chi(T,t)$ with t for $T>270$ K$\approx T_{ps}$ (not shown) indicates that a significant time is required for the sample to reach internal thermal equilibrium even for $T>T_{ps}$.

IV. ANALYSIS AND DISCUSSION

A. The approach of the susceptibility of quenched $La_2CuO_{4.044}$ towards equilibrium

To provide initial insight into the kinetics leading to the time dependence of $\chi(t)$ for $La_2CuO_{4.044}$ after quenching and increasing T to the measurement temperatures in Fig. 6, it is useful to consider the approach of $\chi(t)$ to equilibrium normalized by the difference between χ at the start of the measurement at a particular T and the equilibrium value. Thus, let us define the fractional approach to equilibrium for $H=5$ T by

$$f(t)=\frac{\chi(t)-\chi(t=0)}{\chi^{SLC}-\chi(t=0)},$$

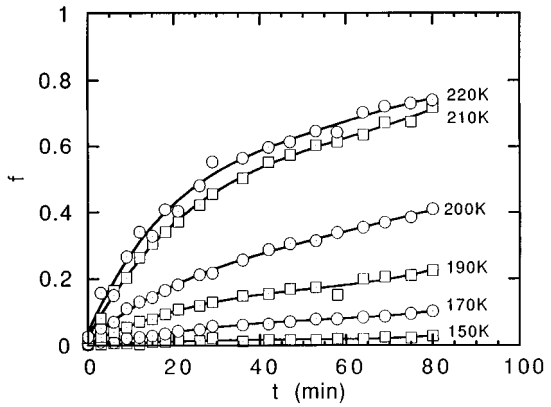

FIG. 7. The function $f(t)=[\chi(t)-\chi(t=0)]/[\chi^{\mathrm{SLC}}-\chi(t=0)]$ versus time t, showing the fractional approach of the susceptibility $\chi(t)$ towards equilibrium. For clarity, only a representative fraction of the data is shown.

where χ^{SLC} is the equilibrium value at a particular temperature as determined upon slowly cooling the sample (see Fig. 5). The function $f(t)$ is plotted in Fig. 7, where it is seen that the normalized rate of approach to equilibrium increases monotonically with increasing T from 150 up to 220 K. This implies that the diffusion rate of the excess oxygen also increases monotonically with T over this T range.

B. Oxygen diffusion during phase separation in $La_2CuO_{4+\delta}$: A model for the time dependence of the magnetic susceptibility at fixed temperature

In this section, we derive a phenomenological model for analyzing the above time (t)-dependent susceptibility data, from which we derive the temperature-dependent diffusion coefficient of the excess oxygen and the diffusion coefficient activation energy. One expects the linear size S of the oxygen-rich domains to initially increase during phase separation as a power law in t, $S\sim t^x$, where the exponent is $x\approx 1/3$ to $1/2$ for a system such as ours with a conserved order parameter.[55] Therefore, if the diffusion resulting in phase separation is effectively one dimensional (1D), the number N_2 of excess oxygen atoms in the oxygen-rich phase should initially scale as $N_2\sim t^x$, whereas if the diffusion is two dimensional (2D), $N_2\sim t^{2x}$. Thus, including both 1D and 2D cases, we expect that N_2 should initially grow as $N_2\sim t^{1/3}$ to $N_2\sim t$. We wish to synthesize a model which contains the initial power-law time dependence, allows consideration of both 1D and 2D diffusion, and which explicitly contains the diffusion coefficient.

We begin by closely following the treatment of Shewmon.[56] One may describe the oxygen drift flux J_{dr} driven by the phase separation as $J_{\mathrm{dr}}=c\mathbf{v}_{\mathrm{dr}}=c\mu F$, where c is the excess oxygen concentration, μ and $\mathbf{v}_{\mathrm{dr}}$ are, respectively, the mobility and drift velocity of the excess oxygen, and $F=-\boldsymbol{\nabla}V$ is a generalized force driving the phase separation and which is associated with the potential V. The Einstein relation relates μ to the diffusion constant D of a random walk as $\mu=D/k_BT$. Thus, one obtains

$$J_{\mathrm{dr}}=c\mathbf{v}_{\mathrm{dr}}=\frac{-Dc\boldsymbol{\nabla}V}{k_BT}. \tag{1}$$

Since the phase-separation process causes an accumulation of oxygen, an opposing diffusion flux, $J_{\mathrm{diff}}=-D\boldsymbol{\nabla}c$, is induced according to Fick's first law. The total flux of excess oxygen is the sum of the drift flux and the diffusion flux,

$$J=J_{\mathrm{diff}}+J_{\mathrm{dr}}=-D(\boldsymbol{\nabla}c+c\boldsymbol{\nabla}V/k_BT). \tag{2}$$

Inserting Eq. (2) into the continuity equation $\partial c/\partial t=-\boldsymbol{\nabla}\cdot\mathbf{J}$ yields a differential equation for $c(\mathbf{r},t)$:[56]

$$\frac{\partial c}{\partial t}=D\boldsymbol{\nabla}(\boldsymbol{\nabla}c+c\boldsymbol{\nabla}V/k_BT). \tag{3}$$

One can obtain a closed-form expression for $c(\mathbf{r},t)$ if we neglect the influence of $\boldsymbol{\nabla}c$.[55] This assumption appears to be justified because the phase-separation process in $La_2CuO_{4+\delta}$ is diffusion limited.[9] Then Eq. (3) becomes

$$\frac{\partial c}{\partial t}=cD\,\frac{\boldsymbol{\nabla}^2V}{k_BT}. \tag{4}$$

The solution is

$$c(\mathbf{r},t)=c_0\exp\left(Dt\,\frac{\boldsymbol{\nabla}^2V}{k_BT}\right), \tag{5}$$

where c_0 is the (uniform) excess oxygen concentration prior to phase separation.

Knowledge of $V(\mathbf{r})$ is necessary to obtain a solution for $c(\mathbf{r},t)$ in Eq. (5). In an analysis of 3D stress-assisted precipitation, Shewmon has shown that the concentration of precipitated regions has a $t^{2/3}$ time dependence for $V(\mathbf{r})=-\beta/r$ in the short time limit where $\boldsymbol{\nabla}V$ is dominant and $\boldsymbol{\nabla}c\approx 0$.[56] Here, we extend this calculation to 1D and 2D segregation. For 1D diffusion, we assume the general form

$$\frac{dV(\mathbf{r})}{dr}=\frac{\epsilon}{x_0}\left(\frac{x_0}{r}\right)^{\alpha},\quad \text{in 1D}, \tag{6a}$$

where x_0 is an arbitrary scale length and r is the distance from the potential core line. In 2D, we assume that

$$V(r)=\frac{-\gamma}{r^{2\alpha}},\quad \text{in 2D}, \tag{6b}$$

where $\gamma>0$ is a constant and r is the radial distance of an excess oxygen atom from the potential core. In Eqs. (6), the power α determines the initial time dependence of the number of excess oxygen atoms in the oxygen-rich phase during phase separation (see below), and these postulated forms for $V(\mathbf{r})$ were chosen in order to obtain the same [see Eq. (9) below] time dependences for a given α in the 1D and 2D cases. We now assume that the area A from which the excess oxygen diffuses to a potential core is finite in extent, as would occur if there is a regular array of identical potential cores. This assumption is consistent with the herringbone pattern of phase-separated regions in $La_2CuO_{4+\delta}$ observed in Ref. 9; these micrographs also suggest that the 1D diffusion model may be more appropriate than the 2D one. In 1D, let $A=Lr_0$, where L is the length of the potential core line and r_0 is the transverse dimension of the area A. In 2D, let $A=\pi r_0^2$, where r_0 is now the radius of the area A. For the 1D and 2D potentials suggested above in Eqs. (6), one obtains

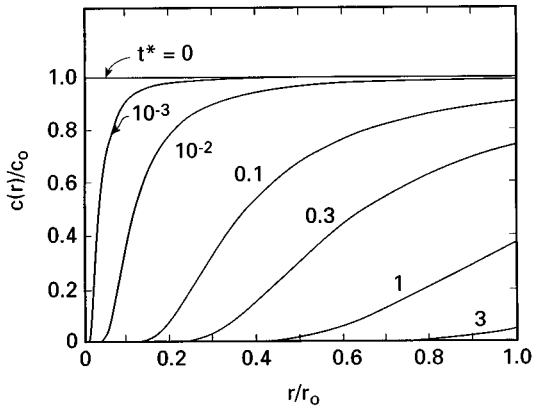

FIG. 8. Excess oxygen concentration c, divided by the uniform concentration c_o prior to phase separation, versus distance r divided by r_o, where r is the transverse distance from the potential core line and r_o is the maximum transverse distance per potential core line. These are plots of the prediction in Eq. (7a) of our model for the 1D case with $\alpha=1$, for various values of the reduced time $t^*=(CD/k_BT)t$.

$$c(r,t)=\frac{N_2(t)}{A}\,\delta(r)+c_o\exp\left(\frac{-CDtr_o^{(\alpha+1)}}{k_BTr^{(\alpha+1)}}\right),\quad \text{in 1D} \tag{7a}$$

and

$$c(r,t)=\frac{N_2(t)}{A}\,\delta(r)+c_o\exp\left(\frac{-CDtr_o^{2(\alpha+1)}}{k_BTr^{2(\alpha+1)}}\right),\quad \text{in 2D,} \tag{7b}$$

where $N_2(t)$ is the number of excess oxygen atoms in the oxygen-rich δ_2 phase at time t, i.e., in the potential core, $\delta(r)$ is the Dirac delta function and $C=\epsilon\alpha/r_o^{1+\alpha}x_o^{1-\alpha}$ for the 1D case and $C=4\gamma\alpha^2/r_o^{2(\alpha+1)}$ for the 2D case. From Eqs. (7), phase separation proceeds by the unphysical accumulation of excess oxygen on a potential core line (in 1D) or a potential core point (in 2D) at $r=0$, which would correspond to infinite density. Physically, one reinterprets N_2 to be the number of phase separated atoms present at the physically realized density of the δ_2 phase.[56] This accumulation depletes the region around the potential core of excess oxygen atoms until, at long times, there are no excess oxygen atoms outside of the potential core. Examples of the concentration profiles outside of the potential core versus r for various t for the 1D case with $\alpha=1$ from Eq. (7a) are shown in Fig. 8. Thus, in this model the equilibrium ($t=\infty$) concentration of excess oxygen atoms in the oxygen-poor δ_1 phase is zero. Were it not for the freezing of the excess oxygen atoms below ~150 K, the left edge of the miscibility gap in the equilibrium phase diagram might approach $\delta_1=0$, in contrast to the presumably nonequilibrium behavior seen below ~150 K in Fig. 1.

Since the total number N of excess oxygen atoms associated with each potential core is constant ($N=c_oA$), one can obtain $N_2(t)$ by integrating the exponential term in Eqs. (7) as in Fig. 8 out to the edge of the region containing the potential core (i.e., to $r=r_o$), and subtracting this result from the total number N of excess oxygen atoms:

$$N_2(t)=Lc_o\int_0^{r_o}\left[1-\exp\left(\frac{-CDtr_o^{(\alpha+1)}}{k_BTr^{(\alpha+1)}}\right)\right]dr,\quad \text{in 1D} \tag{8a}$$

and

$$N_2(t)=\pi c_o\int_0^{r_o^2}\left[1-\exp\left(\frac{-CDtr_o^{2(\alpha+1)}}{k_BTr^{2(\alpha+1)}}\right)\right]dr^2,\quad \text{in 2D.} \tag{8b}$$

After changing variables to $u=[CDtr_o^{(\alpha+1)}/k_BTr^{(\alpha+1)}]^{1/2}$ in the 1D case and $u=[CDtr_o^{2(\alpha+1)}/k_BTr^{2(\alpha+1)}]^{1/2}$ in the 2D case, and normalizing to the equilibrium number, $N_2(t=\infty)=N=c_oLr_o$ in 1D and $N=c_o\pi r_o^2$ in 2D, of excess oxygen atoms in the oxygen-rich phase, one obtains for both the 1D and 2D cases

$$\frac{N_2(t)}{N_2(\infty)}=\frac{2}{\alpha+1}\,(CDt/k_BT)^{1/(\alpha+1)}\times\int_{(CDt/k_BT)^{1/2}}^{\infty}\frac{1-\exp(-u^2)}{u^{(\alpha+3)/(\alpha+1)}}\,du. \tag{9}$$

For $CDt/k_BT\ll 1$, Eq. (9) predicts an initial time dependence $N_2(t)/N_2(\infty)\sim(CDt/k_BT)^{1/(\alpha+1)}$, whereas for $CDt/k_BT\gg 1$, $N_2(t)/N_2(\infty)\to 1$. From the introduction to this section, we wish to examine values of α such that the initial $N_2(t)\sim t^y$ with $y=1/(\alpha+1)=1/3$ to 1, corresponding to $\alpha=2$ to 0. Note that the time parameter t at a particular temperature T is the time since phase segregation started for an ideally quenched sample, as determined at that T. However, our quenched sample is already partially phase separated (see below), and the degree of phase separation at the beginning of a $\chi(t)$ measurement at fixed T increases with T because of the sequential order of the measurements. Therefore, to fit to our experiments, we replace t in Eq. (9) by t_o+t, where the latter t is the measured time elapsed at a particular T:

$$\frac{N_2(t)}{N_2(\infty)}=\frac{2}{\alpha+1}\,[CD(t_o+t)/k_BT]^{1/(\alpha+1)}\times\int_{[CD(t_o+t)/k_BT]^{1/2}}^{\infty}\frac{1-\exp(-u^2)}{u^{(\alpha+3)/(\alpha+1)}}\,du. \tag{10}$$

The parameter t_o is the time it would have taken at temperature T for the sample to phase separate from an ideally quenched state to the actual extent present in the sample at the beginning of a $\chi(t)$ measurement at that T. A plot of $N_2(t_o+t)/N_2(\infty)$ versus $CD(t_o+t)/k_BT$ from Eq. (10) with $\alpha=1$ ($x=1/2$) is shown as the solid curve in Fig. 9. The parameters t_o and product CD are to be adjusted to obtain a fit of the data to the solid curve (see below).

At this point we must specify how to relate $N_2(t_o+t)/N_2(\infty)$ in Eq. (10) to the measured time-dependent susceptibility $\chi(t_o+t)$ at a particular T. To do this, we assume that at any given t and T the sample consists of uniform fractions N_1/N of the δ_1 phase, N_2/N of the δ_2 phase with the remainder being untransformed δ phase; this is an approximation to the concentrations in the model as discussed above and shown in Fig. 8. At a given t and T, the measured susceptibility χ is then

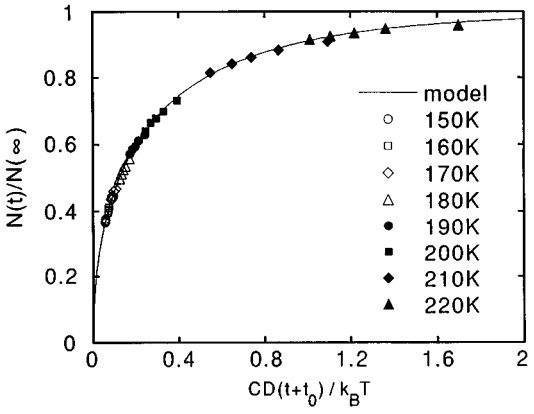

FIG. 9. Time (t) dependence of the number $N_2(t)$ of excess oxygen atoms in the oxygen-rich δ_2 phase in phase-separated $La_2CuO_{4+\delta}$ normalized to the equilibrium value $N_2(t=\infty)$. An ideal quench is assumed at time $t+t_o=0$. The solid curve is the prediction of our model in Eq. (10) with $\alpha=1$, and the data points are fits of the data in Figs. 5–7 to the curve using Eq. (13); for clarity, only a few representative data points are plotted.

$$\chi=\frac{N_1}{N}\chi_1+\frac{N_2}{N}\chi_2+\left(1-\frac{N_1+N_2}{N}\right)\chi_x, \tag{11}$$

where χ_1, χ_2, and χ_x are the molar susceptibilities of the respective pure phases at temperature T. Equation (11) implicitly assumes that the susceptibilities of the δ_1, δ_2, and untransformed δ phases are independent of particle size, shape, and edge width, which are not necessarily good approximations in view of the data for $La_2CuO_{4.044}$ in Fig. 2(a). However, we have no information on these particle properties below T_{ps} or the dependences of the susceptibilities on them with which to refine the model. By combining Eq. (11) with the oxygen atom conservation expression $N_1\delta_1+N_2\delta_2=(N_1+N_2)\delta$, one obtains

$$\chi-\chi_x=\frac{N_2}{N}\left[\left(\frac{\delta_2-\delta}{\delta-\delta_1}\right)(\chi_1-\chi_x)+\chi_2-\chi_x\right] \tag{12}$$

and, at the time of $t=t_o+t$ and $t=\infty$ from Eq. (12), the desired form

$$\frac{\chi(t_o+t)-\chi_x}{\chi^{SLC}-\chi_x}=\frac{N_2(t_o+t)}{N(\infty)}, \tag{13}$$

where $\chi^{SLC}\equiv\chi(t=\infty)$ is the equilibrium susceptibility in Fig. 5 obtained upon slowly cooling the sample.

The ideal quenched susceptibility χ_x in Eq. (13) for $La_2CuO_{4.044}$ is estimated to be that of an equivalently hole-doped sample of $La_{2-x}Sr_xCuO_4$. In the low doping regime ($\delta\lesssim0.08$) of $La_2CuO_{4+\delta}$, each excess oxygen appears to donate about one hole to the CuO_2 planes,[22,27,35,41] in contrast to two holes/excess oxygen atom expected for O^{-2}. Consistent with the former hole-doping assignment, $\chi_x(T)$ for $La_{2-x}Sr_xCuO_4$ with $x=0.04$,[57] is in close agreement with $\chi(T)$ for $La_2CuO_{4.044}$ above $T_{ps}\approx270$ K, as shown by the lower solid curve in Fig. 5(a). Further, comparison of the data at ~100 K for $La_2CuO_{4.044}$ with those for $La_{1.96}Sr_{0.04}CuO_4$ in Fig. 5(b) shows that our quenching procedure does not result in an ideal quench for $La_2CuO_{4.044}$.

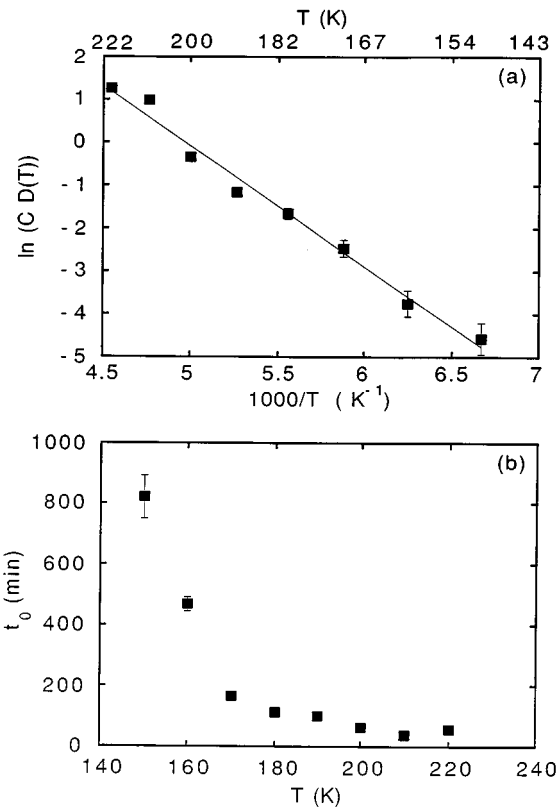

FIG. 10. (a) Product of the constant C and the diffusion constant D for the excess oxygen in $La_2CuO_{4.044}$, versus inverse temperature ($1/T$), and (b) the parameter t_o versus T. The parameters CD and t_o were obtained by fitting the data in Figs. 5–7 to the model calculation in Eqs. (10) and (13) (solid curve in Fig. 9).

We illustrate our data fitting procedure for the value $\alpha=1$. Using Eq. (13), the $\chi^{SLC}(T)$ data and the $\chi_x(T)$ for $x=0.04$ in Fig. 5(b), we determined the constant t_o and the product CD in Eq. (10) at each T which allowed the data for $H=5$ T at each fixed T in Figs. 5–7 to be scaled onto the solid curve in Fig. 9. The scaled data are plotted in Fig. 9, and the fitting parameters CD and t_o are plotted versus $1/T$ and T in Figs. 10(a) and 10(b), respectively. In Fig. 10(b), the value of t_o is seen to increase with decreasing T, which is expected since the oxygen mobility decreases with decreasing T. From Fig. 10(a), the diffusion constant D of the excess oxygen atoms shows an activated temperature dependence with a nearly temperature-independent activation energy $E_a=(2810\pm20)$ K$=0.234$ eV. Similar analyses with $\alpha=0$, 0.5, and 2 yielded $E_a=2457$, 2582, and 3155 K, respectively. Since the actual effective dimensionality of the oxygen diffusion during phase separation in $La_2CuO_{4+\delta}$ is unclear, we conclude that within our model, the activation energy is $E_a=(2800\pm350)$ K$=(0.24\pm0.03)$ eV. Analysis of 0.5 T data as in Figs. 5–7 as above gave good agreement with the model, with the same value of E_a to within the given error bar and similar $t_o(T)$ values as in Fig. 10(b). Our value for E_a is comparable with the rough estimate between 200 and 250 K (0.25 eV) obtained in a ^{139}La NQR study of high-pressure-oxygenated $La_2CuO_{4+\delta}$ with $\delta\approx0.03$,[18] which together with our result suggests a similar activation energy for diffusion from 150 K up to at least 250 K. We note, however, that the data in Figs.

10(a) and 10(b) suggest a possible anomaly at ~210 K in the temperature-dependent diffusion coefficient and t_o values.

C. Comparison of the above oxygen diffusion properties in $La_2CuO_{4+\delta}$ with those inferred from other probes

The above $\chi(t,T)$ results in Figs. 5–7 indicate that after quenching to 5 K, phase separation in $La_2CuO_{4.044}$ is first observable with increasing T at 140–150 K. This result is consistent with the structural data in the phase diagram in Fig. 1, where the sides of the miscibility gap first begin to deviate from the vertical above ~150 K. Our result is also consistent with the high precision resistivity data of Ryder *et al.*,[9] which first exhibit resolved hysteresis between slowly cooled and heated samples above ~150 K, and with the detailed studies of Kremer and co-workers for $\delta \lesssim 0.02$,[39–41] in which the first increase in the apparent superconducting volume fraction of quenched samples occurred above ~150 K.

From Fig. 7, the normalized phase-separation rate increases monotonically with increasing T from 150 to 220 K. From our modeling of these data in Fig. 9 using Eqs. (10) and (13), we confirmed that the diffusion constant for the diffusing species giving rise to the phase separation increases with T, and obtained a nearly temperature-independent diffusion coefficient activation energy $E_a = (0.24 \pm 0.03)$ eV from 150 to 220 K, with the exception of a possible anomaly near 210 K. We conclude that the same species (excess oxygen atoms) is responsible for phase separation and its influence on the physical properties throughout this T range. This conclusion is in agreement with that of Ref. 9, but is in contrast to a previous suggestion (see Introduction) that diffusion of ferrons *without* concurrent oxygen diffusion occurs below ~200 K in initially quenched samples with $\delta \lesssim 0.02$.[39–41]

In ^{139}La and ^{63}Cu NMR/NQR studies of lightly doped $La_2CuO_{4+\delta}$, an enhanced nuclear relaxation rate due to motion of the excess oxygen is observed only above ~200 K.[15,43,58–63] Since we have concluded that the rate of excess oxygen diffusion increases continuously above 150 K, the observation of relaxation in the NMR/NQR measurements due to oxygen motion only above ~ 200 K is evidently due to the fact that the time scale of our $\chi(t,T)$ measurements is $\sim 10^9$ times longer than that of NMR/NQR. To illustrate, the oxygen-induced ^{139}La NQR/NMR relaxation above 200 K for samples with $\delta \lesssim 0.01$ has been quantitatively explained using a two-dimensional (2D) oxygen self-diffusion and random-walk model.[60,61] These measurements indicate a 2D self-diffusion constant which follows the relation $D = (0.067\ \mathrm{cm^2/s})\exp(-5000\ \mathrm{K}/T)$.[61] On a $t = 1$ h time scale, the calculated diffusion length $\sqrt{Dt}$ is 60 μm at 200 K and 90 Å at 150 K. The value at 150 K is clearly large enough to influence the superconducting and magnetic properties even though the NMR/NQR measurements are not sensitive to oxygen diffusion at this T.

One should bear in mind that many previous studies of the thermal history dependence of the physical properties were carried out on $La_2CuO_{4+\delta}$ samples with $\delta \lesssim 0.02$, whereas most of our data are for $\delta = 0.044$. From Fig. 1, the latter composition has a different ambient temperature structure than the former one, and may have a different excess oxygen diffusion behavior during phase separation. Consistent with this possibility, the activation energy of 5000 K for 2D excess oxygen self-diffusion cited above for $\delta \lesssim 0.01$ (Ref. 61) is ≈70% larger than we find for $\delta = 0.044$. Oxygen diffusion studies to lower doping levels would be of interest in this regard.

D. Thermal history dependence of the superconducting properties of phase-separated $La_2CuO_{4+\delta}$

Previous interpretations of the thermal history dependence of the superconducting properties invariably implicitly assumed that they were related to the phase separation process. However, in Fig. 3, we demonstrated that a suppression of T_c of the pure superconducting $\delta_2 = 0.065$ phase by ≈2 K occurs upon quenching compared to slowly cooling, even though this is a single phase to 10 K. This thermal history dependence is presumably associated with variations in the nature and degree of crystallographic ordering of the excess oxygen atoms, as reflected by the occurrence of superstructure reflections in neutron-diffraction[35] and transmission-electron microscopy[23,64] measurements. Consistent with this scenario, the pressure dependence of T_c for the δ_2 phase depends on the temperature at which the pressure is changed.[44] Thus, a significant fraction of the reduction in T_c of phase-separated $La_2CuO_{4+\delta}$ samples due to quenching appears to arise from behavior intrinsic to the pure δ_2 phase.

Several workers have found that following a quench, T_c for $\delta \approx 0.03$ shows a maximum for annealing temperatures T_{ann} around 200 K,[13,15,18,42,43] which is significantly below the phase-separation temperature T_{ps} (see Fig. 1). Again, this behavior may be in part associated with thermal history-dependent oxygen ordering effects within the δ_2 phase. An additional factor may be the spatial variation in the excess oxygen content in phase-separated samples. The above analysis indicated that the drift rate of the excess oxygen and the rate of phase separation decrease rapidly with decreasing T below T_{ps}. On the other hand, the opposing diffusion flux [the first term on the right-hand side of Eq. (2), which was neglected in the above analysis] tends to restore the system to a uniform oxygen concentration. This diffusion flux would tend to make the oxygen concentration within the oxygen-rich δ_2 domains inhomogeneous, particularly near the domain boundaries, and decrease the domain size. These effects of the diffusion flux would decrease with decreasing T. Below ~150–200 K, however, oxygen diffusion becomes limited and the phase-separation process is arrested. The optimum T_c obtained for $T_{ann} \approx 200$ K is probably associated with both enhanced oxygen ordering in, and optimized size and homogeneity of, the oxygen-rich superconducting δ_2 domains.[65,66]

Our quenching procedures appear to be very similar to those by Kremer and co-workers in Refs. 39–41; however, our samples show a much smaller influence of the thermal treatment on the Meissner effect than those with $\delta \lesssim 0.02$ studied by Kremer *et al.*, suggesting that oxygen diffusion at a given T is faster in our samples with $\delta = 0.030$ and 0.044 than in theirs with $\delta \lesssim 0.02$ (see above), and/or that flux pinning is weaker for $\delta = 0.044$. Similar to our results in Fig. 3(a), the Meissner fraction of high-pressure-oxygenated $La_2CuO_{4+\delta}$ crystals with $\delta \approx 0.03$ is relatively large and is insensitive to T_{ann} following a quench.[13,18,42]

E. Mechanism for phase separation

Based on a t-J model calculation, chargeless doped holes in a CuO_2 plane of the high superconducting transition temperature (T_c) cuprates do not have a uniform density. Rather, they are predicted to separate into a hole-rich metallic phase and a hole-deficient insulating phase below a certain critical doping concentration, thereby minimizing the antiferromagnetic (AF) bond-breaking energy.[67,68] For macroscopic phase separation to occur and not to be frustrated by the long-range Coulomb interaction between the doped holes, the dopant ions must phase separate along with the doped holes in order to compensate the holes' charge.[69] From Fig. 6, we inferred that $T_{ps} > T_N$ in $La_2CuO_{4.044}$, as was also found from NMR and neutron-diffraction results on high-pressure-oxygenated $La_2CuO_{4+\delta}$ single crystals.[13,48] This inequality is further confirmed by the large difference between the maximum $T_{ps} \approx 415$ K (Ref. 30) and maximum $T_N = 325-328$ K (Refs. 6, 31, 32, and 47) reported for the $La_2CuO_{4+\delta}$ system. The apparent observation that $T_{ps} < T_N$ (Refs. 8 and 10) for some samples with compositions apparently just to the right of the left miscibility gap boundary (see Fig. 1) is the exception rather than the rule. Thus, long-range AF ordering cannot be a significant driving force for phase separation below T_{ps}, since in that case one would always expect $T_{ps} < T_N$. Indeed, the magnetic (electronic) mechanism for phase separation[67–69] only requires the presence of dynamic two-dimensional short-range AF order, rather than three-dimensional long-range AF order. Elastic forces may also be important to phase separation in $La_2CuO_{4+\delta}$ as in other cases of spinodal decomposition.[9,70]

Although macroscopic phase separation is prevented in the Sr-doped $La_{2-x}Sr_xCuO_4$ system because the Sr^{+2} ions are immobile and cannot phase separate along with the doped holes, dynamic nanoscopic inhomogeneities in the doped-hole concentration are still expected from the electronic scenario for phase separation.[69] Indeed, recent ^{139}La NQR and $\chi(T)$ measurements provided evidence for an inhomogeneous doped-hole distribution in lightly doped $La_{2-x}Sr_xCuO_4$ ($x \leq 0.08$), where the doped holes were concluded to segregate into walls separating weakly coupled hole-poor AF domains; the domain size $L \sim 10-100$ Å was inferred to decrease with increasing x.[34,57,71–73] Similar conclusions have been made for the $RBa_2Cu_3O_{7-\delta}$ materials.[1,2] These observations provide indirect support for an electronic contribution to the mechanism for phase separation in the $La_2CuO_{4+\delta}$ system. Experimental studies of the thermal history dependence of the physical properties such as the present work and the works cited above are now sufficiently detailed to warrant quantitative theoretical predictions of these properties for the various mechanisms proposed for phase separation. Such quantitative study is necessary to definitively establish whether the phase separation is driven primarily by an electronic or elastic mechanism.

ACKNOWLEDGMENTS

The authors thank F. Borsa, R. J. Birgeneau, J. D. Jorgensen, M. A. Kastner, P. G. Radaelli, and M. C. Tringides for valuable discussions, and L. L. Miller for experimental assistance. The work at M.I.T. was supported primarily by the MRSEC Program of the National Science Foundation under Award No. 94-00334. Ames Laboratory is operated for the U.S. Department of Energy by Iowa State University under Contract No. W-7405-Eng-82. The work at Ames was supported by the Director for Energy Research, Office of Basic Energy Sciences.

[1] *Phase Separation in Cuprate Superconductors*, edited by K. A. Müller and G. Benedek (World Scientific, Singapore, 1993).

[2] *Phase Separation in Cuprate Superconductors*, edited by E. Sigmund and K. A. Müller (Springer-Verlag, Heidelberg, 1994).

[3] For a recent review, see D. C. Johnston, F. Borsa, P. C. Canfield, J. H. Cho, F. C. Chou, L. L. Miller, D. R. Torgeson, D. Vaknin, J. Zarestky, J. Ziolo, J. D. Jorgensen, P. G. Radaelli, A. J. Schultz, J. L. Wagner, S-W. Cheong, W. R. Bayless, J. E. Schirber, and Z. Fisk, in *Phase Separation in Cuprate Superconductors* (Ref. 2), pp. 82–100.

[4] J. D. Jorgensen, B. Dabrowski, S. Pei, D. G. Hinks, L. Soderholm, B. Morosin, J. E. Schirber, E. L. Venturini, and D. S. Ginley, Phys. Rev. B **38**, 11 337 (1988).

[5] B. Dabrowski, J. D. Jorgensen, D. G. Hinks, S. Pei, D. R. Richards, H. B. Vanfleet, and D. L. Decker, Physica C **162-164**, 99 (1989).

[6] S-W. Cheong, M. F. Hundley, J. D. Thompson, and Z. Fisk, Phys. Rev. B **39**, 6567 (1989). The anomalies in the normal-state properties assigned in this paper to the antiferromagnetic transition were later apparently concluded in Ref. 7 to be due to the phase-separation transition (see also, Ref. 9).

[7] M. F. Hundley, J. D. Thompson, S-W. Cheong, Z. Fisk, and J. E. Schirber, Phys. Rev. B **41**, 4062 (1990).

[8] M. F. Hundley, R. S. Kwok, S-W. Cheong, J. D. Thompson, and Z. Fisk, Physica C **172**, 455 (1991).

[9] J. Ryder, P. A. Midgley, R. Exley, R. J. Beynon, D. L. Yates, L. Afalfiz, and J. A. Wilson, Physica C **173**, 9 (1991).

[10] M. Yamada and Y. Oda, Solid State Commun. **76**, 1337 (1990).

[11] L. L. Miller, K. Sun, D. C. Johnston, J. E. Schirber, and Z. Fisk, J. Alloys Compounds **183**, 312 (1992).

[12] P. C. Hammel, A. P. Reyes, Z. Fisk, M. Takigawa, J. D. Thompson, R. H. Heffner, S-W. Cheong, and J. E. Schirber, Phys. Rev. B **42**, 6781 (1990).

[13] P. C. Hammel, E. T. Ahrens, A. P. Reyes, J. D. Thompson, D. E. MacLaughlin, Z. Fisk, P. C. Canfield, and J. E. Schirber, in *Phase Separation in Cuprate Superconductors* (Ref. 1), pp. 139–157. The stated miscibility gap boundaries below ~200 K ($\delta_1 \approx 0.01$ and $\delta_2 \approx 0.08$) were later corrected in Refs. 15 and 18 below to be $\delta_1 \approx 0.01$ and $\delta_2 \approx 0.06$.

[14] P. C. Hammel, A. P. Reyes, S-W. Cheong, Z. Fisk, and J. E. Schirber, Phys. Rev. Lett. **71**, 440 (1993).

[15] P. C. Hammel, A. P. Reyes, E. T. Ahrens, D. E. MacLaughlin, J. D. Thompson, Z. Fisk, P. C. Canfield, S-W. Cheong, and J. E. Schirber, Physica B **199&200**, 235 (1994).

[16] C. Chaillout, S-W. Cheong, Z. Fisk, M. S. Lehmann, M. Marezio, B. Morosin, and J. E. Schirber, Physica C **158**, 183 (1989).

[17] C. Chaillout, J. Chenavas, S-W. Cheong, Z. Fisk, M. Marezio, B. Morosin, and J. E. Schirber, Physica C **170**, 87 (1990).
[18] A. P. Reyes, P. C. Hammel, E. T. Ahrens, J. D. Thompson, P. C. Canfield, Z. Fisk, and J. E. Schirber, J. Phys. Chem. Solids **54**, 1393 (1993).
[19] A. Wattiaux, J-C. Park, J-C. Grenier, and M. Pouchard, C. R. Acad. Sci. **310**, 1047 (1990).
[20] J-C. Grenier, A. Wattiaux, N. Lagueyte, J-C. Park, E. Marquestaut, J. Etourneau, and M. Pouchard, Physica C **173**, 139 (1991).
[21] R. Suryanarayanan, O. Gorochov, M. S. R. Rao, L. Ouchammou, W. Paulus, and G. Heger, Physica C **185-189**, 573 (1991); R. Suryanarayanan, W. Paulus, M. S. R. Rao, O. Gorochov, L. Ouhammou, and G. Heger, Supercond. Sci. Technol. **5**, 82 (1992).
[22] F. C. Chou, J. H. Cho, and D. C. Johnston, Physica C **197**, 303 (1992).
[23] J-C. Grenier, N. Lagueyte, A. Wattiaux, J-P. Doumerc, P. Dordor, J. Etourneau, M. Pouchard, J. B. Goodenough, and J. S. Zhou, Physica C **202**, 209 (1992); J-C. Grenier, A. Wattiaux, and M. Pouchard, in *Phase Separation in Cuprate Superconductors* (Ref. 1), pp. 187–207.
[24] P. Rudolf, W. Paulus, and R. Schöllhorn, Adv. Mater. **3**, 438 (1991).
[25] N. Casañ-Pastor, P. Gomez-Romero, A. Fuertes, J. M. Navarro, M. J. Sanchis, and S. Ondoño, Physica C **216**, 478 (1993).
[26] D. C. Johnston, F. Borsa, J. H. Cho, F. C. Chou, D. R. Torgeson, D. Vaknin, J. L. Zarestky, J. Ziolo, J. D. Jorgensen, P. G. Radaelli, A. J. Schultz, J. L. Wagner, and S-W. Cheong, J. Alloys Compounds **207/208**, 206 (1994).
[27] J. C. Grenier, F. Arrouy, J. P. Locquet, C. Monroux, M. Pouchard, A. Villesuzanne, and A. Wattiaux, in *Phase Separation in Cuprate Superconductors* (Ref. 2), pp. 236–256.
[28] J.-S. Zhou, H. Chen, and J. B. Goodenough, Phys. Rev. B **50**, 4168 (1994).
[29] F. C. Chou, D. C. Johnston, S-W. Cheong, and P. C. Canfield, Physica C **216**, 66 (1993).
[30] P. G. Radaelli, J. D. Jorgensen, R. Kleb, B. A. Hunter, F. C. Chou, and D. C. Johnston, Phys. Rev. B **49**, 6239 (1994).
[31] O. Schärpf and H. Capellmann, Z. Phys. B **80**, 253 (1990).
[32] T. Thio and A. Aharony, Phys. Rev. Lett. **73**, 894 (1994).
[33] D. C. Johnston, S. K. Sinha, A. J. Jacobson, and J. M. Newsam, Physica C **153-155**, 572 (1988).
[34] J. H. Cho, F. C. Chou, and D. C. Johnston, Phys. Rev. Lett. **70**, 222 (1993).
[35] P. G. Radaelli, J. D. Jorgensen, A. J. Schultz, B. A. Hunter, J. L. Wagner, F. C. Chou, and D. C. Johnston, Phys. Rev. B **48**, 499 (1993).
[36] R. Yoshizaki, H. Sawada, T. Iwazumi, and H. Ikeda, Physica C **153-155**, 1495 (1988); Solid State Commun. **65**, 1539 (1988); Synth. Met. **29**, F735 (1989).
[37] A. Sulpice, P. Lejay, R. Tournier, B. Chevalier, G. Demazeau, and J. Etourneau, Physica B **165&166**, 1157 (1990). These results did not confirm the magnetic-field effect on the Meissner fraction reported in Ref. 36.
[38] Y. Oda and M. Yamada, Physica C **178**, 158 (1991).
[39] R. K. Kremer, E. Sigmund, V. Hizhnyakov, F. Hentsch, A. Simon, K. A. Müller, and M. Mehring, Z. Phys. B **86**, 319 (1992).
[40] R. K. Kremer, V. Hizhnyakov, E. Sigmund, A. Simon, and K. A. Müller, Z. Phys. B **91**, 169 (1993).
[41] R. K. Kremer, A. Simon, E. Sigmund, and V. Hizhnyakov, in *Phase Separation in Cuprate Superconductors* (Ref. 2), pp. 66–81.
[42] E. T. Ahrens, A. P. Reyes, P. C. Hammel, J. D. Thompson, P. C. Canfield, Z. Fisk, and J. E. Schirber, Physica C **212**, 317 (1993).
[43] P. C. Hammel, A. P. Reyes, E. T. Ahrens, Z. Fisk, P. C. Canfield, J. D. Thompson, and J. E. Schirber, in *Phase Separation in Cuprate Superconductors* (Ref. 2), pp 185–198.
[44] J. E. Schirber, W. R. Bayless, F. C. Chou, D. C. Johnston, P. C. Canfield, and Z. Fisk, Phys. Rev. B **48**, 6506 (1993).
[45] M. Mehring, M. Baehr, P. Gergen, J. Groβ, C. Kessler, and N. Winzek, in *Phase Separation in Cuprate Superconductors* (Ref. 1), pp. 67–84.
[46] G. Wübbeler and O. F. Schirmer, Phys. Status Solidi (B) **174**, K21 (1992); O. F. Schirmer, G. Wübbeler, and Th. Wahlbrink, in *Phase Separation in Cuprate Superconductors* (Ref. 2), pp. 133–141.
[47] J. Saylor, L. Takacs, C. Hohenemser, J. I. Budnick, and B. Chamberland, Phys. Rev. B **40**, 6854 (1989).
[48] D. Vaknin, J. L. Zarestky, D. C. Johnston, J. E. Schirber, and Z. Fisk, Phys. Rev. B **49**, 9057 (1994).
[49] S-W. Cheong, Z. Fisk, J. O. Willis, S. E. Brown, J. D. Thompson, J. P. Remeika, A. S. Cooper, R. M. Aikin, D. Schiferl, and G. Gruner, Solid State Commun. **65**, 111 (1988).
[50] H. Nishihara, N. Sugh, Y. Hidaka, M. Oda, T. Shimizu, H. Yasuoka, K. Koga, K. Kishio, K. Kitazawa, K. Fueki, M. Suzuki, T. Murakami, and T. Ohtani, J. Phys. Soc. Jpn. **57**, 1159 (1988).
[51] A. N. Bazhan and V. N. Bevz, Superconductivity **4**, 100 (1991).
[52] Y. J. Uemura, W. J. Kossler, J. R. Kempton, X. H. Yu, H. E. Schone, D. Opie, C. E. Stronach, J. H. Brewer, R. F. Kiefl, S. R. Kreitzman, G. M. Luke, T. Riseman, D. Ll. Williams, E. J. Ansaldo, Y. Endoh, E. Kudo, K. Yamada, D. C. Johnston, M. Alvarez, D. P. Goshorn, Y. Hidaka, M. Oda, Y. Enomoto, M. Suzuki, and T. Murakami, Physica C **153-155**, 769 (1988).
[53] K. Yamada, E. Kudo, Y. Endoh, Y. Hidaka, M. Oda, M. Suzuki, and T. Murakami, Solid State Commun. **64**, 753 (1987).
[54] For a review, see D. C. Johnston, J. Magn. Magn. Mater. **100**, 218 (1991).
[55] M. C. Tringides, Phys. Rev. Lett. **65**, 1372 (1990); R. Yamamoto and K. Nakanishi, Phys. Rev. B **49**, 14 958 (1994); G. Leptoukh, B. Strickland, and C. Roland, Phys. Rev. Lett. **74**, 3636 (1995), and references cited.
[56] P. G. Shewmon, *Diffusion in Solids* (McGraw-Hill, New York, 1963), p. 23.
[57] J. B. Torrance, A. Bezinga, A. I. Nazzal, T. C. Huang, S. S. P. Parkin, D. T. Keane, S. J. LaPlaca, P. M. Horn, and G. A. Held, Phys. Rev. B **40**, 8872 (1989); T. Nakano, M. Oda, C. Manabe, N. Momono, Y. Miura, and M. Ido, *ibid*. **49**, 16 000 (1994).
[58] F. C. Chou, F. Borsa, J. H. Cho, D. C. Johnston, A. Lascialfari, D. R. Torgeson, and J. Ziolo, Phys. Rev. Lett. **71**, 2323 (1993).
[59] J. Ziolo, F. Borsa, M. Corti, and A. Rigamonti, Physica C **153-155**, 725 (1988).
[60] A. Lascialfari, F. Borsa, P. Ghigna, D. R. Torgeson, J. Ziolo, F. Chou, and D. C. Johnston, J. Phys. Condens, Matter **5**, B 19 (1993).
[61] S. Rubini, F. Borsa, P. Canfield, F. C. Chou, Q. Hu, A. Lascialfari, D. C. Johnston, A. Rigamonti, and D. R. Torgeson, Physica C **235-240** 1717 (1994).
[62] T. Imai, C. P. Slichter, K. Yoshimura, and K. Kosuge, Phys. Rev. Lett. **70**, 1002 (1993).
[63] M. Mehring, P. Gergen, C. Kessler, and S. Krämer, in *Phase Separation in Cuprate Superconductors* (Ref. 2), pp. 165–184.

[64] E. Takayama-Muromachi, T. Sasaki, and Y. Matsui, Physica C **207**, 97 (1993).
[65] M. Itoh, T. Huang, J. D. Yu, Y. Inaguma, and T. Nakamura, Phys. Rev. B **51**, 1286 (1995).
[66] T. Kyômen, M. Oguni, M. Itoh, and J. D. Yu, Phys. Rev. B **51**, 3181 (1995).
[67] V. J. Emery, S. A. Kivelson, and H. Q. Lin, Phys. Rev. Lett. **64**, 475 (1990).
[68] S. A. Kivelson, V. J. Emery, and H. Q. Lin, Phys. Rev. B **42**, 6523 (1990).
[69] V. J. Emery and S. A. Kivelson, Physica C **209**, 597 (1993).
[70] J. W. Cahn, Acta Metall. **9**, 795 (1961).
[71] J. H. Cho, F. Borsa, D. C. Johnston, and D. R. Torgeson, Phys. Rev. B **46**, 3179 (1992).
[72] F. Borsa, P. Carretta, A. Lascialfari, D. R. Torgeson, F. C. Chou, and D. C. Johnston, Physica C **235-240**, 1713 (1994).
[73] F. Borsa, P. Carretta, J. H. Cho, F. C. Chou, Q. Hu, D. C. Johnston, A. Lascialfari, D. R. Torgeson, R. J. Gooding, N. M. Salem, and K. J. E. Vos, Phys. Rev. B **52**, 7334 (1995).